Chapter 5

Eigenvalue and Stability Analysis

The eigenvalue based state space stability and the participation factor analysis are two of the main areas of focus in this chapter. This chapter begins with a brief description of certain preliminaries significant to this analysis. The rest of the chapter contains the implementation of the eigenvalue analysis for AC and DC microgrid small signal models and their simulation results obtained in MATLAB. A Lypunov based mathematical stability formulation for DC microgrid reduced order equivalent has been included at the end of this chapter.

5.1 Preliminaries

Few of the preliminary concepts and definitions significant to the eigenvalue analysis of microgrid model are presented in this section.

5.1.1 Eigenvalue

For an *n* by *n* linear system's state matrix $\boldsymbol{A}$, the roots of the characteristic equation (5.1) are called its Eigenvalues [91-92]. Alternatively, eigenvalues are scalar parameter for which a non-zero solution of equation (5.2) exists.

$$\det(\boldsymbol{A} - \boldsymbol{\lambda I}) = 0 \tag{5.1}$$

$$\boldsymbol{A\phi} = \boldsymbol{\lambda\phi} \tag{5.2}$$

where, $\boldsymbol{\phi}$ is an n by 1 vector.

Eigenvalues can be real or complex conjugate pair. Real eigenvalues correspond to non-oscillatory modes whereas, complex conjugate pair corresponds to oscillatory modes. For the oscillatory eigenvalues of the form; $\lambda = \sigma \pm j\omega$; positive value of σ gives an increasing function in time and negative value gives a decaying function with time. Further, the damping ratio of oscillation is derived from real part of eigenvalues and the frequency of oscillation is determined from its imaginary part.

$$\xi = \frac{-\sigma}{\sqrt{\sigma^2+\omega^2}} \; ; f = \frac{\omega}{2\pi} \tag{5.3}$$

5.1.2 Eigenvector

An eigenvector is a characteristic vector of state matrix $\boldsymbol{A}$; such that its magnitude depends on the multiplication of state matrix and eigenvalues. The eigenvectors are of two types; right eigenvector and left eigenvector [74].

Right eigenvector is a non-zero vector $\boldsymbol{\phi_r}$, that satisfies the equation, $\boldsymbol{A\phi_r = \lambda\phi_r}$. Whereas, left eigenvector is a non-zero vector $\boldsymbol{\phi_l}$, such that, $\boldsymbol{\phi_l A = \phi_l \lambda}$. These eigenvectors are orthogonal when they correspond to different eigenvalues. Assume ϕ_{ri} is associated with λ_i and $\boldsymbol{\phi_{lj}}$ is associated with λ_j, then, $\boldsymbol{\phi_{ri}\phi_{lj}} = 0$.

For right and left eigenvectors corresponding to same eigenvalue, their product is a non-zero quantity. For normalised eigenvectors;

$$\boldsymbol{\phi_{ri}\phi_{li}} = 1 \tag{5.4}$$

5.1.3 Modal Matrix

Defining matrices associated with left eigenvectors, right eigenvectors and eigenvalues as; $\boldsymbol{\phi_R}$, $\boldsymbol{\phi_L}$ and $\boldsymbol{\Lambda}$ respectively which have n elements [75]; given as;

$$\boldsymbol{\phi_R} = \begin{bmatrix} \boldsymbol{\phi_{R1}} \\ \boldsymbol{\phi_{R2}} \\ \boldsymbol{\phi_{R3}} \\ . \\ \boldsymbol{\phi_{Rn}} \end{bmatrix}; \boldsymbol{\phi_L} = [\boldsymbol{\phi_{L1}} \quad \boldsymbol{\phi_{L2}} \quad \boldsymbol{\phi_{L3}} \quad .. \quad \boldsymbol{\phi_{Ln}}]; \boldsymbol{\Lambda} = \begin{bmatrix} \lambda_1 & 0 & 0 & 0 \\ 0 & \lambda_2 & 0 & 0 \\ 0 & 0 & . & 0 \\ 0 & 0 & 0 & \lambda_n \end{bmatrix}$$

Thus equation (5.2) and (5.4) can be rewritten as;

$$\boldsymbol{\phi_R \phi_L = I \Rightarrow \phi_R^{-1} = \phi_L}$$

$$\boldsymbol{A\phi_R = \Lambda\phi_R}$$

Then the modal matrix is defined as; $\boldsymbol{\phi_R A \phi_R^{-1} = \Lambda}$. (5.5)

5.1.4 Eigenvalue Sensitivity

Eigenvalue sensitivity quantifies the sensitivity of the ith eigenvalue to the kth state in a system where *i=k*. This analysis helps determine the faulty or undesirable eigenvalues associated to uncontrolled or unstable states which can be eliminated or relocated to improve the dynamical system response.

Finding the derivative of equation (5.5) w.r.t. a_{ki} element in the kth row and jth column of $\boldsymbol{A}$ and using the orthogonal and characteristic equations; the resultant equation is;

$$\phi_{li} \frac{\partial \boldsymbol{A}}{\partial a_{ki}} \phi_{ri} = \frac{\partial \lambda_i}{\partial a_{ki}}$$

But the value of $\frac{\partial \boldsymbol{A}}{\partial a_{ki}}$ is zero except for at the element in kth row and jth column; thus

$$\phi_{Lik}\phi_{Rji} = \frac{\partial \lambda_i}{\partial a_{ki}} \tag{5.6}$$

Thus, the sensitivity of eigenvalue λ_i to element a_{ki} is the product of left eigenvector element and right eigenvector elements.

5.1.5 Participation Matrix

The participation matrix determines the relation between mode and state by using the combined knowledge from right and left eigenvectors. It is defined as;

$$\boldsymbol{P} = [\boldsymbol{p_1}\ \boldsymbol{p_2}\ \boldsymbol{p_3} \dots \dots \boldsymbol{p_n}]$$

$$p_i = \begin{bmatrix} p_{i1} \\ p_{i2} \\ p_{i3} \\ . \\ p_{in} \end{bmatrix} = \begin{bmatrix} \phi_{Li1}\phi_{R1i} \\ \phi_{Li2}\phi_{R2i} \\ \phi_{Li3}\phi_{R3i} \\ . \\ \phi_{Lin}\phi_{Rni} \end{bmatrix} \tag{5.7}$$

The element $p_{ik} = \phi_{Lik}\phi_{Rki}$ is called the participation factor and gives a measure of the participation of kth state in ith mode and vice versa. Participation factor analysis is crucial to system stability concern and is extensively been used in power system applications to determine the contribution or influence of a specific state variable to a specific mode for various system design requirements.

5.1.6 State Space Stability

Stability analysis in control systems in the form of their state space representations can easily be determined by the location of the eigenvalues in complex s-plane [92-93]. For a linearized state space representation, the transfer function is defined as;

$$G(s) = \boldsymbol{C}(s\boldsymbol{I} - \boldsymbol{A})^{-\mathbf{1}}\boldsymbol{B} + \boldsymbol{D} = \boldsymbol{C}\frac{adj(s\boldsymbol{I}-\boldsymbol{A})}{|s\boldsymbol{I}-\boldsymbol{A}|}\boldsymbol{B} + \boldsymbol{D} \tag{5.8}$$

Thus, the poles of $G(s)$ corresponds to the roots of $|s\boldsymbol{I} - \boldsymbol{A}|$ which is the characteristic polynomial as discussed in Section 5.1.1. Hence, the poles of the transfer function are the system eigenvalues and so, the location of these eigenvalues help determine system stability for all control applications. In the s domain, it is required that

all the poles of the system be located in the left-half plane, and therefore all the eigenvalues of $\boldsymbol{A}$ must have negative real parts.

Moreover, with respect to the condition for BIBO stability which demands a bounded output for every bounded input to the system over the time period of $[t_0, \infty)$, a positive eigenvalue would result in system state approaching infinity with time approaching infinity. As the system output is scaled version of system state, thus this unbounded system state will cause the output to become unbounded and so, the system becomes unstable. Thus, it can be summed up that the system is stable if the eigenvalues of state matrix $\boldsymbol{A}$ have negative real parts [94].

5.2 Eigenvalue Analysis of AC Microgrid

The eigenvalue analysis of AC microgrid model has been divided into two parts: Eigenvalue and stability analysis of autonomous mode and Eigenvalue and stability analysis of grid-tied mode as below.

5.2.1 Eigenvalue and stability analysis of autonomous mode

For the state space model of the AC microgrid developed in Section 3.2.2 in Chapter 3 with 36 states and four input variables as in (3.43-3.44), the eigenvalues of the linearized state space representation with their major participating state variables obtained through participation matrix are enlisted in Table 5.1.

As seen from this table, a total of 16 oscillatory/non-oscillatory modes are identified. As discussed earlier in this Section 5.1.1, an oscillatory mode corresponds to a complex conjugate pair of eigenvalues and non-oscillatory mode corresponds to an eigenvalue on real axis of s-plane. Thus, the states representing output voltage and current

in both d and q axis, i.e., v_{odq}, i_{odq}, are observed to be highly oscillatory with frequencies of up to 1995 Hz approximately. The lowest frequency of 0.005 Hz is in Mode 13 whose major contributors are active and reactive powers of the inverters, P_{12}, Q_{12} .

Table 5.1. Eigenvalues and participation analysis in autonomous AC microgrid.

Eigenvalues	**Real part ± jImaginary part**		**Damping ratio, ξ**	**Damped frequency, f_i(Hz)**	**Mode**		**Highest Contributors**
					Oscillatory	**Non-Oscillatory**	
3,4	-2500.554	12528.618	0.1958	1995.0030	1		v_{oq1}, i_{oq1}
5,6	-2499.782	12526.573	0.1957	1994.6773	2		v_{oq2}, i_{oq2}
7,8	-2321.497	11784.723	0.1933	1876.5483	3		v_{od1}, i_{od1}
9,10	-2317.907	11780.499	0.1930	1875.8757	4		v_{od2}, i_{od2}
11	-7912.594	0	1			14	$v_{od1,f}$
12	-7903.629	0	1			15	$v_{od2,f}$
1,2	-375	376.6084	0.7056	59.9695	5		i_{lineDQ}
13,14	-3333.330	376.6084	0.9937	59.9695			$i_{loadDQ2}$
15,16	-1666.666	376.6084	0.9754	59.9695			$i_{loadDQ1}$
19,20	-258.0320	64.1104	0.9705	10.2087	6		i_{ldq2}
17.18	-257.5532	60.9617	0.9731	9.7073	7		i_{ldq1}
21,22	-79.3639	16.5199	0.9790	2.6306	8		γ_{dq1}
23,24	-77.3698	19.2989	0.9703	3.0731	9		γ_{dq2}
25,26	**-10.6101**	**7.8436**	**0.8041**	**1.2490**	**10**		$\boldsymbol{\delta_2, \emptyset_{PLL2}}$
27,28	**-0.4722**	**6.0420**	**0.0779**	**0.9621**	**11**		$\boldsymbol{\emptyset_{dq1}}$
29,30	**-1.2883**	**4.6232**	**0.2684**	**0.7362**	**12**		$\boldsymbol{\emptyset_{dq2}}$
31	**-2.1209**	**0**	**1**			**16**	$\boldsymbol{\emptyset_{PLL1}}$
32,33	**-50.2448**	**0.0308**	**0.9999**	**0.0049**	**13**		$\boldsymbol{P_{12}, Q_{12}}$
34,35	-50.2515	0.0315	0.9999	0.0050			
36	0	0					δ_1

Dominant eigenvalues have been highlighted in this table.

For eigenvalues with damping ratios from 0 to 1, i.e., underdamped dynamics, the settling time is inversely proportional to damping ratios and hence, lower ξ, corresponds to higher settling time. The damping ratios of the complex eigenvalues demonstrate the damped oscillations which die out and gives a stable overall system dynamics. Moreover,

from the point of view of state space stability, the negative real part of eigenvalues confirm the stable performance of the microgrid model.

Further, the reduced order modelling of the microgrid model with dominant pole dynamics as discussed in Chapter 4, system's reduced order model retains the eigenvalues with smallest real part. Thus, for a 9^{th} order reduction, the corresponding modes that can be considered are; mode 10, 11, 12, 13 and 16 (Table 5.1). Fast modes die out quickly in the system response, whereas, the slower mode's effect predominates throughout in response. Since these modes are slow with larger time constants as compared to the other modes, the overall reduced order response will be similar to the original system response, with negligible inaccuracies, mainly in the initial period of the response. The impact of the major state variables in these modes combined, obtains the system response in reduced order. The quantitative analysis of the various state contributors in the retained oscillatory modes, i.e. Mode 10, 11, 12 and 13, are presented as bar graph in Figure 5.1. Although the angle deviation of inverter 1 is considered as a slow state at origin, its small- signal response during both the transient and the steady state is zero. This state is thus ignored in subsequent analysis, when the reduced order system is being developed.

To gain a deeper insight into the stability consideration with respect to deviations in the system dynamics in reduced order modelling, a state perturbation analysis has been carried out. The state perturbation in the small signal model of microgrid system causes the eigenvalues to deviate from their values calculated by linearization of the system about a steady state operating point. The small perturbation in the eigenvalues will be insignificant for fast modes, as a change of 0.001 Hz will not change their dynamics much, but, for the slower modes, a change of 0.001 Hz will significantly increase the time constant of the system.

Table 5.2. shows the effect of perturbation on low-frequency eigenvalues. The changes in damping ratios and frequencies on these modes thereby changes the overall system response under perturbation. Significant parameter or load changes may even effect the stability of the overall system.

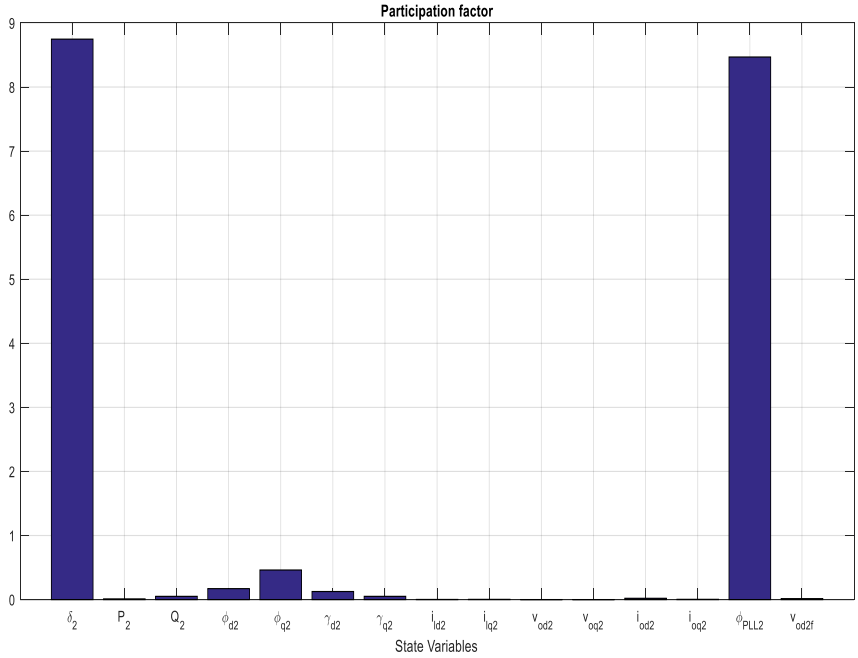

(a)

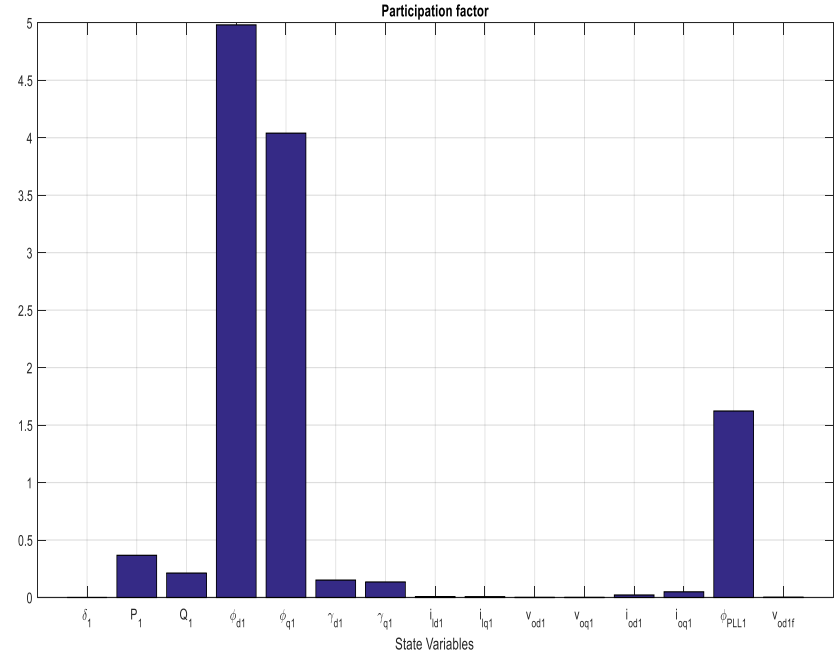

(b)

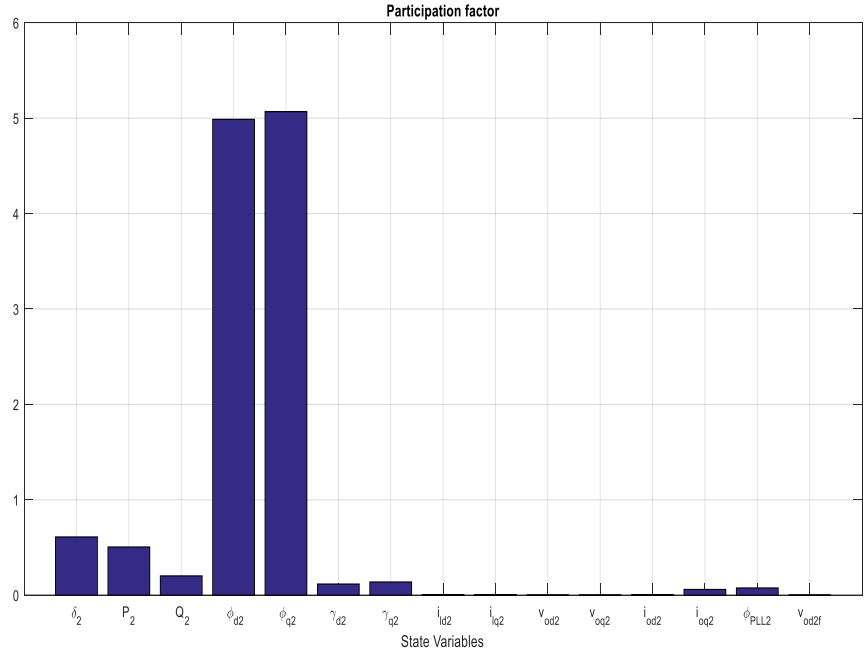

(c)

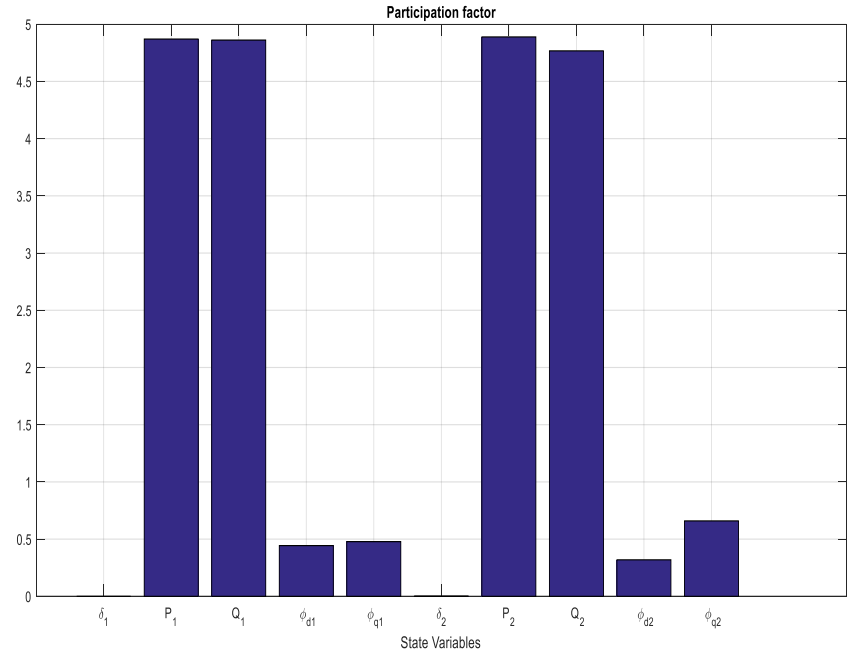

(d)

Figure 5.1. *Bar graph representation of participation factors in AC microgrid in autonomous mode.(a) mode 10 (b) mode 11 (c) mode 12 (d) mode 13 (Reduced order oscillatory modes).*

Cases 1 and 2, in this Table 5.2, demonstrate two different levels of uncertainty, wherein, the comparatively larger perturbation in case 2 makes the system unstable by the movement of the smallest real-valued mode toward the unstable region of s-plane. The state perturbation in this case, results in a net negative damping in the overall system and frequencies as low as 0.002 Hz. Due to small uncertainties considered in the system, the relative participation of states in different mode will not change and so, it is not re-evaluated in this work.

Considering a general perturbation in the system which may be due to parameter changes, changes in operating conditions etc., the effect of subsequent state perturbation on the full order and reduced order system have been critically analysed by considering their effects on the slower modes, as the deviations in the fast modes will not impact the system dynamical behaviour. Cases 1 and 2 in Table 5.2 demonstrate two different perturbations on the state space model wherein, the later one alters the system stability.

Therefore, the eigenvalue analysis of the 36^{th} order AC microgrid model in autonomous mode with state perturbation in its 9^{th} order reduced equivalent gives a detailed insight into the system stability and the efficiency in system modelling.

5.2.2 Eigenvalue and stability of Grid-tied mode

An analysis similar to that for AC microgrid in autonomous mode has been carried out for grid-tied mode wherein, the 15^{th} order complex model is reduced to its 2^{nd} order equivalent with dominant dynamics. The state space model in Section 3.2.3 in Chapter 3 has been derived as a 15^{th} order model with 2 inputs as the reference active and reactive powers. Table 5.3 gives the eigenvalues of the state space model and also enlists the various state contributors.

Table 5.2. Effect of perturbation on slow modes.

Indices	***λ***	***λ +Δ λ***		***Damping ratio***			***Damped freq.(Hz)***		
		CASE 1	**CASE 2**	ξ_{λ}	$\xi_{\lambda+\Delta\lambda}{}^{1}$	$\xi_{\lambda+\Delta\lambda}{}^{2}$	f_{λ}	$f_{\lambda+\Delta\lambda}{}^{1}$	$f_{\lambda+\Delta\lambda}{}^{2}$
25,26	-10.6101±j7.8436	-10.6204±j7.8297	-10.7297±j7.6884	0.804	0.805	0.813	1.249	1.247	1.224
27,28	-0.4722±j6.0420	-0.4732±j6.0419	0.0144±j4.6165	0.078	0.078	-0.003	0.962	0.962	0.735
29,30	-1.2883±j4.6232	-1.2785±j4.6296	-1.2521±j2.6654	0.268	0.266	0.425	0.736	0.737	0.424
31	-2.1209±j0	-2.1207±j0	-3.0613±j0	1	1	1			
32,33	-50.2448±j0.0308	-50.2515±j0.0235	-50.2532±j0.0130	0.999	0.999	0.999	0.005	0.004	0.002

A modal analysis reveals that the Mode 1 and 2 are the oscillating modes with frequency of oscillation of 1773.59 Hz and 1803.63 Hz respectively. The participation factors determine the participating states in these modes as i_{odq}, v_{odq}.Therefore, the system dynamics owes its oscillations to the voltages and currents in dq axis on the output side of the inverter. The other modes only contribute to the damping in the overall system dynamics.

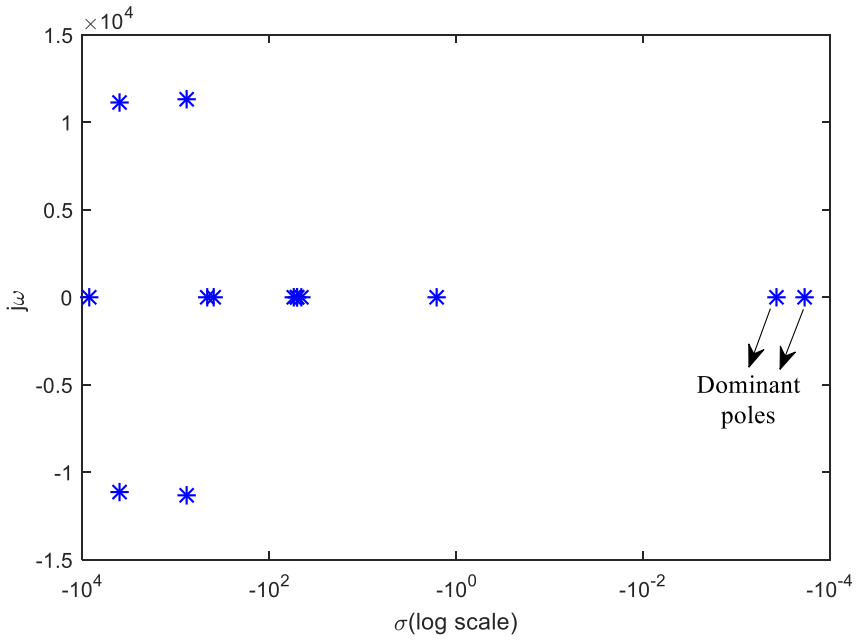

Figure 5.2. *Eigenvalue Plot of AC microgrid in grid-tied mode.*

Further, a stability analysis with the eigenvalues obtained from their state space representation as in the Table 5.3 suggest a stable system dynamical response due to the location of all the system poles in the left half of s-plane. A diagrammatic representation of eigenvalues in an eigenvalue plot in Figure 5.2. presents the location of eigenvalues and the roots closest to the imaginary axis in s-plane.

Table 5.3. Eigenvalues and participation analysis in grid-tied AC microgrid.

Eigenvalue indices	Real part	Imaginary part	Damped freq. (Hz)	Mode		Highest Contributors	Significant Contributors
				Oscillatory	Non-oscillatory		
1	0					δ	
2,3	-3999.16	11138.14	1773.59	1		v_{od}	i_{odq}, v_{oq}
4	-8397.40				3	$v_{od,f}$	i_{odq}, v_{odq}
5,6	-765.64	11320.53	1802.63	2		v_{oq}	v_{od}, i_{odq}
7	-462.03				4	i_{ld}	i_{lq}
8	-391.43				5	i_{lq}	i_{ld}
9	-54.61				6	γ_q	γ_d
10	-45.08				7	γ_d	γ_q
11	-50.26				8	Q	
12	-50.26				9	P	
13	-1.63				10	$\emptyset_{PLL}$	
14	**-32.10×10^{-6}**				**11**	**$\emptyset_P$**	
15	**-16.12×10^{-6}**				**12**	**$\emptyset_Q$**	

Dominant eigenvalues have been highlighted in this table.

The reduced order modelling of the grid-tied system by the proposed dominant pole retention method is obtained by retaining modes 11 and 12, due to their dominance over other modes in terms of their proximity to the origin. This can also be observed from the eigenvalue plot in the above Figure 5.2. Thus it can be said that the major influences retained in the reduced order responses are mainly due to the error states from the power controller, $\emptyset_P$, $\emptyset_Q$, which is also demonstrated by the participation factor plot for these two modes in Figure 5.3.

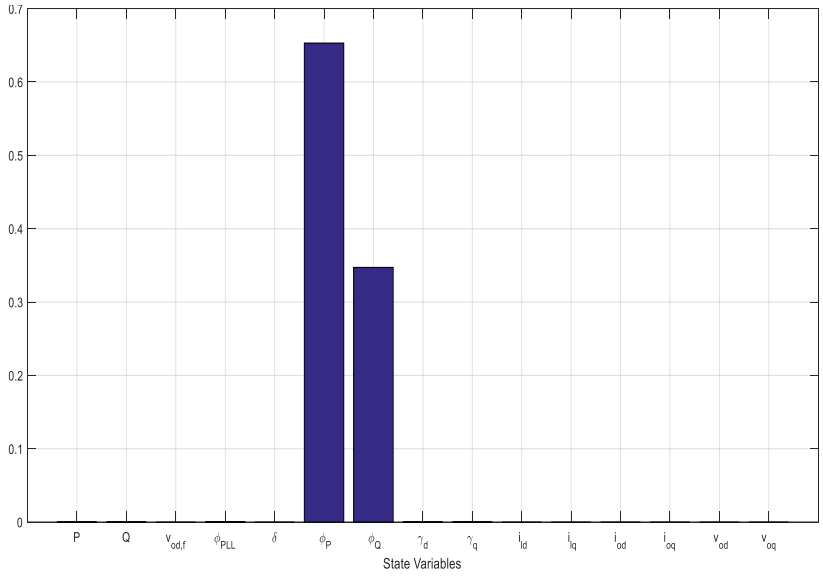

(a)

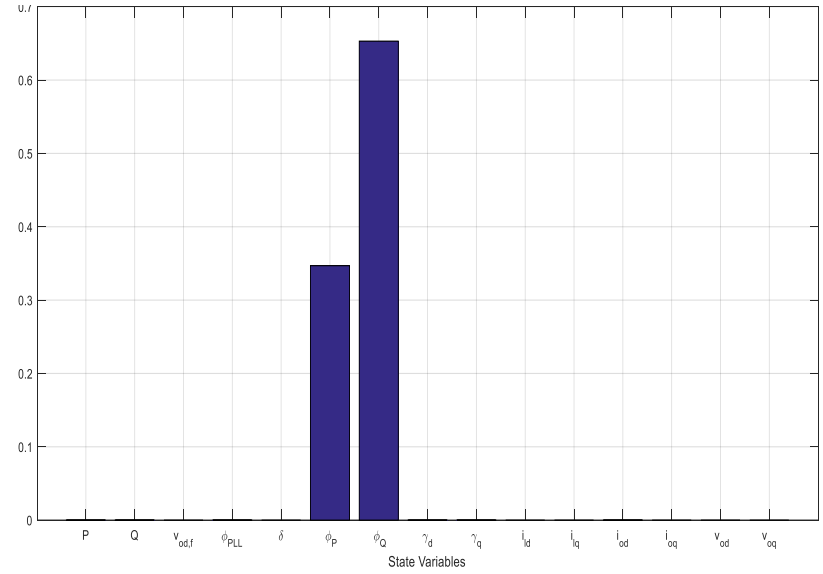

(b)

Figure 5.3. *Bar graph representation of participation factors in AC microgrid in grid-tied mode. (a) Mode 11, (b) Mode 12.*

An enhanced vision of small signal stability in grid-tied mode has been considered with state perturbation in system dynamics with certain fixed changes as in Table 3.1. in Chapter 3. This will affect the location of eigenvalues and thus, may also impact stability. This effect will change the damping and oscillations in the system but the relative

participation of the states in different modes will not change. Thus, the overall impact of states in different modes will remain constant irrespective of small disturbances in the system. Larger perturbations as in case 4 in Section 4 will make the system unstable and hence, their eigenvalue analysis is meaningless.

The eigenvalue and stability analysis of the grid-tied microgrid model of 15^{th} order and its 2^{nd} order equivalent model gives a better understanding of the various aspects such as stability, system responses etc. to be considered in system or controller design.

5.3 Eigenvalue Analysis of DC Microgrid

For the state space model of the higher order and timescale separation based reduced order model of PV-Fuel cell DC microgrid model obtained in Section 3.3 in Chapter 3 and Section 4.2.2 in Chapter 4, the stable system dynamics can be seen from the subsequent eigenvalue plot in Figure 5.4., which shows the full order and reduced order system eigenvalue scatter plot in s-plane. As observed, the eigenvalues of reduced model are closely accumulated around origin and hence appear as a point in s-plane which also contains the largely spread eigenvalues of original system with most of them of large magnitudes and hence comparatively faster dynamics.

The eigenvalues of the 38^{th} order DC microgrid model and its equivalent 12^{th} order model obtained in Chapter 4 are enlisted in Table 5.4. The oscillatory modes in the full order model have been highlighted. The reduced order model can be seen to be a stiff system such that the system response lacks any oscillations in its dynamics.

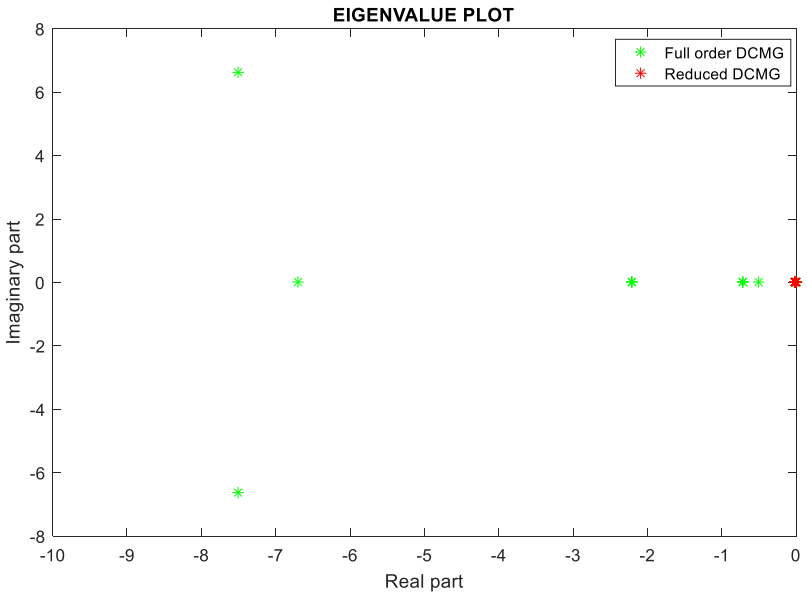

Figure 5.4. *Eigenvalue plot of original and reduced order DC microgrid system.*

A participation factor analysis of dominant mode for fast subsystem is vital to determine the state variable whose influence is expected to be retained in the reduced order model. As discussed in the reduced order modelling of this system in Chapter 4, the slow states are preserved and the most dominant information from fast states is added to the reduced model.

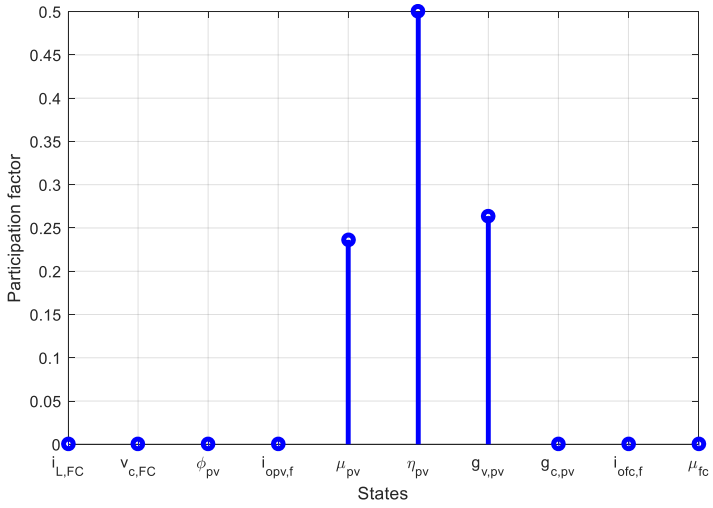

Figure 5.5*. Participation factor of the dominant mode in fast subsystem (-1.36×10^{-11} ± j 5.53×10^{-7})*

Table 5.4. Eigenvalues of full order and reduced order DC Microgrid model.

ORIGINAL (38th ORDER MODEL)		***REDUCED (12th ORDER MODEL)***	
Index	***Eigenvalue***	***Index***	***Eigenvalue***
1	-900.00×10^{-6}	1,2	-1.00×10^{-3}
2	-94.80×10^{-9}	3	-2.80×10^{-3}
3	-1.00×10^{-3}	4	-2.37×10^{-6}
4	-65.42×10^{-6}	5	-14.95×10^{-3}
5	-5.36×10^{3}	6,7,8	-429.49
6	-113.63×10^{3}	9,10,11	-16.67×10^{-3}
7	-25.64×10^{3}	12	-12.32×10^{-3}
8	-1.49×10^{3}		
9	-953.28		
10,11	**-155.43± j320.05**		
12,13	**-139.78± j49.22**		
14,15	-429.49		
16	-6.70		
17,18,19	-2.21		
20	-499.99×10^{-3}		
21,22	**-7.51± j6.62**		
23	-6.15×10^{-12}		
24	-1.11×10^{-3}		
25	-441.93×10^{-6}		
26	-2.31×10^{-3}		
27	-365.40×10^{-6}		
28	-429.49		
29,30,31	-16.67×10^{-3}		
32	-2.99×10^{-6}		
33	-21.24×10^{3}		
34,35	-50.60		
36,37,38	-714.29×10^{-3}		

The major state contributor in the MOR of the fast subsystem by PSO algorithm method can be determined by participation analysis. A participation factor plot of the dominant mode out of the 27 modes in fast subsystem as in equation (4.29) in Chapter 4, has been given in Figure 5.5. This plot indicates the possible state influences that may have been retained in the reduced model obtained. The largest participating state in the dominant mode is η_{pv} and the next large candidates are μ_{pv} and $g_{v,pv}$ which are states associated with PV-droop control. Exact information about states retained in reduced model cannot be attained with this analysis but in a larger sense it can be said that, the reduced order model of fast subsystem preserves the impact of PV-droop control states to a certain extent.

5.4 Lyapunov based Stability Analysis of Reduced Order DC Microgrid System

Following the reduced order modelling of the DC microgrid based on time-scale separation of electrical-nonelectrical states, stability analysis is crucial aspect of small signal modelling and control. In addition to the simpler state space stability analysis as in the previous section, a more accurate and mathematical stability analysis of the DC microgrid system has been obtained in this section. The stability considerations in the DC microgrid under investigation has been discussed in this section in two parts, considering asymptotic stability analysis and an advanced lyapunov based nonlinear stability formulation.

5.4.1 Asymptotic stability of unforced system

Considering the linearized reduced DC microgrid system in general form with 12 states as; $\dot{\boldsymbol{x}} = \boldsymbol{A}\boldsymbol{x}$ with states denoted as; $\boldsymbol{x} = [x_1\ x_2 \dots\dots\dots\dots\dots x_{12}]$ for an unforced system. To investigate the stability of unforced linearized system at origin, according to theorem 1 in Appendix-A, the system matrix is defined as the jacobian matrix at $\boldsymbol{x} = 0$,

as $\boldsymbol{A} = \frac{\partial f_i}{\partial x_i}\Big|_{\boldsymbol{x}=0}$. For the system under consideration, the eigenvalues of the above system matrix formed from state space model as in (25) are given in Table 5.5. As seen from the table, the eigenvalues corresponding to indices 1 to 6, with $Re\ \lambda_i = 0$, can be treated as a special case of theorem 5.1, leading to failure in linearized stability analysis at origin. This results in an incorrect inference of stability and thus, an advanced stability analysis on non-linear system is required.

Table 5.5. Eigenvalues of system matrix, $\boldsymbol{A}$

Index	Real part(eigenvalue)
1,2,3,4,5,6	0
7	-0.0005
8	-0.0022
9	-0.0122
10	-0.0167
11	-0.0167
12	-0.0167

Center manifold theory with its advanced stability analysis can be extracted for the analysis of our system with key theoretical concepts from theorem 2 and 3 as given in Appendix-A for better clarity. The analysis is further simplified by inferring overall system stability from a reduced system with eigenvalues equal to only the zero real eigenvalues of the system.

Step 1: Transformation of A matrix into A_1 and A_2 such that former has zero real eigenvalues and later consists of negative real ones yields two blocks of 6×6 dimensions each. The similarity transformation matrix T is determined from;

$$\boldsymbol{TAT^{-1}} = \begin{bmatrix} \boldsymbol{A_1} & 0 \\ 0 & \boldsymbol{A_2} \end{bmatrix} \tag{5.9}$$

Step 2: The change of state variables from x to y and z, as the zero eigenvalues and negative real eigenvalues subsystems respectively is depicted as;

$$\begin{bmatrix} \boldsymbol{y_{6\times1}} \\ \boldsymbol{x_{6\times1}} \end{bmatrix} = \boldsymbol{T} \begin{bmatrix} x_1 \\ x_2 \\ \vdots \\ x_{12} \end{bmatrix} \tag{5.10}$$

$$\Rightarrow \begin{cases} y_1 = x_5 \\ y_2 = x_6 \\ y_3 = 656x_4 + x_7 \\ y_4 = x_8 \\ y_5 = x_9 \\ y_6 = 22000x_4 + x_{10} \\ z_1 = x_{11} \\ z_2 = x_{12} \\ z_3 = -22000x_4 \\ z_4 = x_1 \\ z_5 = x_2 \\ z_6 = x_3 \end{cases} \tag{5.11}$$

Step 3: Evaluating the state derivatives for the subsystems and presenting in the form as in theorem 5.3;

$$\dot{\boldsymbol{y}} = \boldsymbol{A_1 y} + \boldsymbol{g_1}(\boldsymbol{y}, \boldsymbol{z})$$

$$\dot{\boldsymbol{z}} = \boldsymbol{A_2 z} + \boldsymbol{g_2}(\boldsymbol{y}, \boldsymbol{z}) \tag{5.12}$$

$$\therefore \boldsymbol{A_1} = [0];\ \boldsymbol{A_2} = diag\left(a_r, h_s n_s A_s / M_{fc} C_{fc}, -1/\lambda_C, -1/\lambda_A, -1/\lambda_C\right)$$

$$\boldsymbol{g_1}(\boldsymbol{y}, \boldsymbol{z}) = \boldsymbol{k} z_2;\ \boldsymbol{g_2}(\boldsymbol{y}, \boldsymbol{z}) = [0]$$

where, $\boldsymbol{k}$ is a scalar vector, such that; $\boldsymbol{g_i}(\boldsymbol{y}, \boldsymbol{z})$ are twice continuously differentiability, i.e., $g_i(0,0) = 0;\ \frac{\partial g_i(0,0)}{\partial y} = 0;\ \frac{\partial g_i(0,0)}{\partial z} = 0; i = 1,2.$ (5.13)

Step 4: Assuming center manifold as; $h(y) = z$; as the solution of the partial differential equation defined on h as; $\mathcal{N}\big(h(y)\big) \stackrel{\text{def}}{=} \frac{\partial h}{\partial y}(y)\big(\boldsymbol{k}h(y)\big) - A_2 h(y) = 0$

$$\Rightarrow h(y) = O(|y^2|) \tag{5.14}$$

Thus, the reduced order system becomes; $\dot{\boldsymbol{y}} = O(|y^2|)$ with $\emptyset(y) = 0$.

Step 5: Selecting lyapunov function candidate as the cumulative energy of states, i.e.,

$V(y) = 0.5 \sum y^2 \geq 0 \; \forall \; y \geq 0;$

$$\Rightarrow V(\dot{y}) = \sum y^T \dot{y} = \sum y^T O(|y^2|) \leq \boldsymbol{k}\|y\|_2 \forall \; y \geq 0 \tag{5.15}$$

Thus the reduced '$\boldsymbol{A}$' block subsystem, i.e., system with zero real eigenvalues is asymptotically stable at origin, thus by theorem 3 in Appendix-A, full state unforced system is asymptotically stable at origin.

5.4.2 Input to State Stability (ISS) analysis of nonlinear system

The in-depth investigation of stability of the highly nonlinear DC microgrid with inputs; calls for a lyapunov stability analysis of our system taking the effect of bounded and unbounded inputs into account following theorem 4 in Appendix-A. ISS implies stability of system states to uncontrolled inputs and increased robustness to disturbance inputs. Considering the system to be of the form; $\dot{\boldsymbol{x}} = f(\boldsymbol{x}, \boldsymbol{u})$, selecting system energy as the nonlinear stability function;

$V(x, u) = 0.5 \sum_{i=1}^{12} {x_i}^2 \;\; \forall \; u$

The derivative of $V(x, u)$ along system trajectory is evaluated for robust ISS analysis;

$$V(\dot{x}, u) = \left(-\frac{1}{\lambda_C} {x_1}^2 - \frac{1}{\lambda_A} {x_2}^2 - \frac{1}{\lambda_C} {x_3}^2 - \frac{h_s n_s A_s}{M_{fc} C_{fc}} {x_4}^2 - 2\theta_1 {x_5}^2 - 2\theta_3 {x_6}^2 - \frac{1}{CR} {x_{11}}^2 + a_r {x_{12}}^2 \right) + q(x, u) = -p(x^2) + q(x, u) \tag{5.16}$$

$\forall \; V(\dot{x}, u) \leq 0 \; \exists \; q(x, u) \leq 0$

For $p(x^2) \gg q(x,u)$ so that the negative part is dominant; the lyapunov derivative is redefined as;$V(\dot{x},u) = -(1-\delta)p(x^2) + q(x,u) - \delta p(x^2);\ 0 < \delta < 1$

$$\Rightarrow q(x,u) - \delta p(x^2) \leq 0$$

Thus, equating the state variable coefficients to fulfil the inequality with negligible disturbance input, the resulting constraints on a part of the states are;

$$\left.\begin{aligned} x_5 &\geq \frac{|u_1|}{\delta} \\ x_6 &\geq \frac{|u_2|}{\delta} \\ x_7 &\geq \frac{|u_3|}{\delta} \end{aligned}\right\} \Rightarrow V(\dot{x},u) \leq -(1-\delta)p(x^2)$$

$$\text{i.e. } \begin{aligned} P_{H_2} &\geq \frac{|u_{P_A}|}{\delta} \\ P_{O_2} &\geq \frac{|u_{P_C}|}{\delta} \\ P_{H_2O} &\geq \frac{|u_{T_R}|}{\delta} \end{aligned} \quad \forall\ 0 < \delta < 1 \tag{5.17}$$

Since $V(x,u)$ is positive definite and radially unbounded, hence the overall system is ISS and thus Bounded-Input Bounded-State stability has been mathematically proven. This leads to system states convergence at equilibrium and stability for bounded inputs to the system.

5.5 Summary

In this chapter, the eigenvalue analysis of the state space matrices derived from the state space representations of AC and DC microgrid models obtained in Chapter 3 and their reduced order equivalents obtained in Chapter 4 shows the existence of different modes with their oscillations and damping effects. The participation matrix identifies the contributing state variables of the original system, whose major influences are preserved in the reduced order model. The system stability has also been defined from the location

of these eigenvalues and a case study with certain state perturbations which effect the stability of the microgrid system has also been discussed. Finally, a mathematical analysis of the stability of DC microgrid reduced order system based on Lyapunov functions has been presented to attain more insight into the system stability where the linearization based stability analysis fails. This nonlinear stability analysis of the reduced order model is accomplished through theorems on ISS, ensuring system stability even with uncontrolled disturbance inputs.